Electronic Supplementary Material (ESI) for Catalysis Science & Technology.

Supporting Information

Thermal Synthesis of Electron Deficient Oxygen Species on Crystalline IrO_2

E.A. Carbonio[1,2], F. Sulzmann[2], D. Teschner[2,3], J.J. Velasco-Vélez[2,3,4], M. Hävecker,[1,3] A. knop Gericke[2,3], R. Schlögl[1,2,3], T. Jones[2,5]

[1]Catalysts for Energy, Energy Materials In-situ Laboratory (EMIL), Helmholtz-Zentrum Berlin für Materialien und Energie GmbH, BESSY II, Albert-Einstein-Straße 15, 12489 Berlin, Germany.

[2]Department of Inorganic Chemistry, Fritz-Haber-Institut der Max-Planck-Gesellschaft, Faradayweg 4-6, 14195 Berlin, Germany.

[3]Department of Heterogeneous Reactions, Max Planck Institute for Chemical Energy Conversion, Stiftstraße 34-36, Mülheim an der Ruhr 45470, Germany.

[4]ALBA Synchrotron Light Source, Cerdanyola del Vallés (Barcelona) 08290, Spain.

[5]Theoretical Division, Los Alamos National Laboratory, Los Alamos, New Mexico 87545, United States.

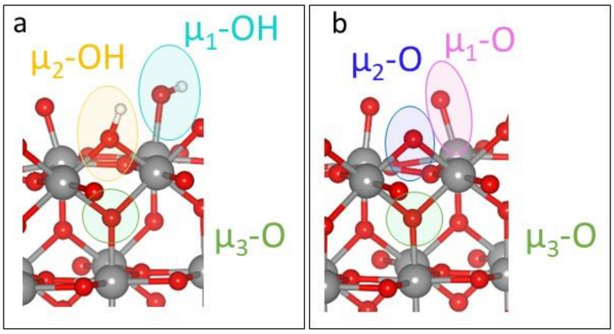

Figure S1. Ball-stick model of IrO_2 (110) surface containing surface oxygen species (a) μ_2-OH and μ_1-OH and (b) μ_2-O and μ_1-O, as indicated by the respective labels. Oxygen atoms are shown as red, iridium grey, and hydrogen white. μ_3-O (lattice oxygen) is also indicated in both panels for comparison.

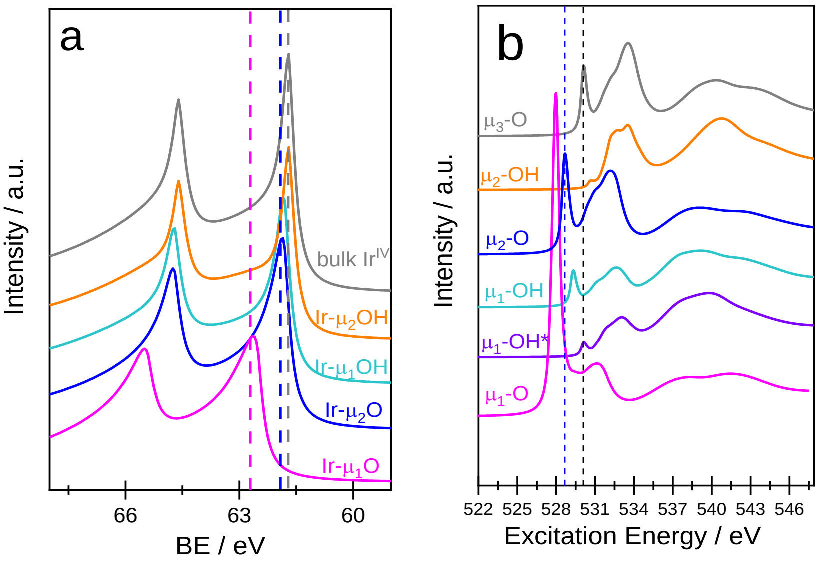

Figure S2. (a) Computed Ir 4f for different surface species on rutile-type IrO_2. Vertical lines indicate the BE corresponding to bulk Ir^{IV}, surface $Ir^{IV+\delta}$ bound to μ_2-O and $Ir^{IV+\delta}$ bound to μ_1-O (b) O K-edges computed at the single particle level. Vertical lines indicate the resonance excitation energy for bulk μ_3-O and surface μ_2-O.

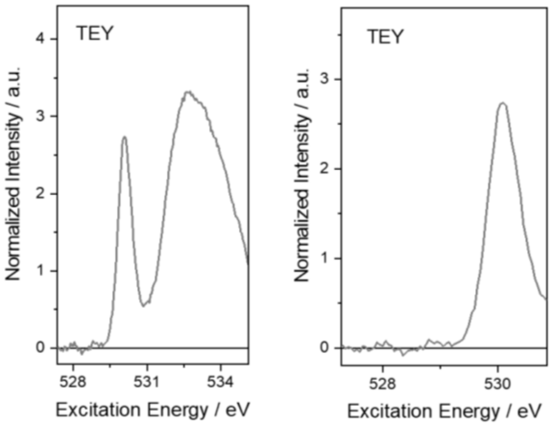

Figure S3. O K-edge (TEY) of calcined IrO_2 as loaded in UHV at RT.

As previously noted, [1] the O K-edge of μ_1-OH is sensitive to the hydrogen bonding environment, with hydrogen bond donating (accepting) μ_1-OH showing a higher (lower) white line and an energy shift. Here we have included two extremes, though under experimental conditions the white line will be an average across all types of accessible H-bonding. This does not change the outcome of this work.

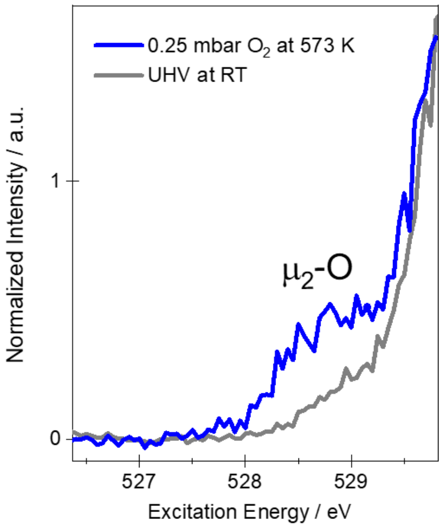

Figure S4. O K-edges (AEY) of IrO_2 (same as in Figure 2b).

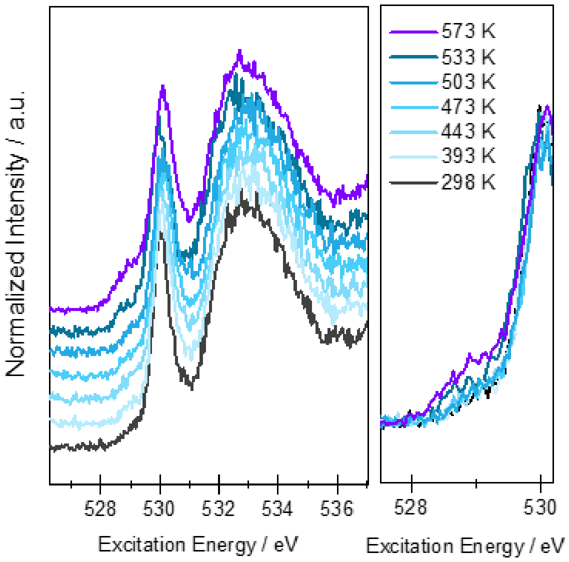

Figure S5. O K-edge spectra (AEY) of calcined IrO_2 under 0.25 mbar O_2 acquired during a temperature ramp (10 $K.min^{-1}$), from 298 K to 573 K.

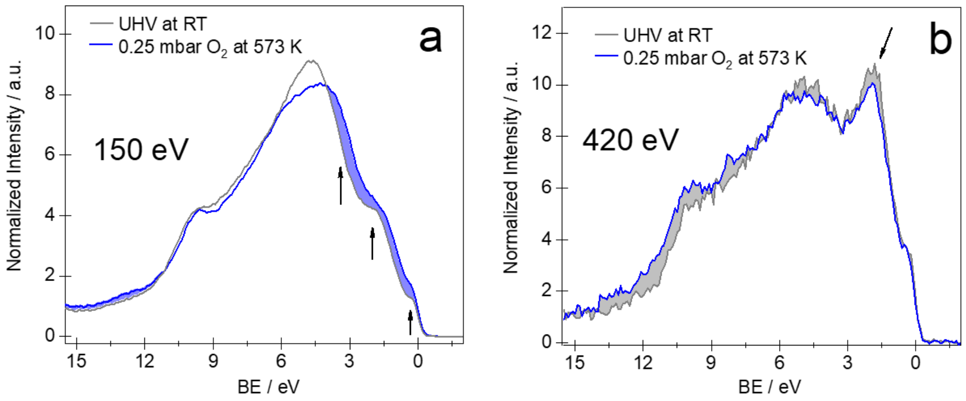

Figure S6. VB measured at 150 eV (a) and 420 eV (b) on rutile-type IrO_2 from Alfa Aesar (calcined) measured for the sample as loaded and under 0.25 mbar O_2 at 573 K.

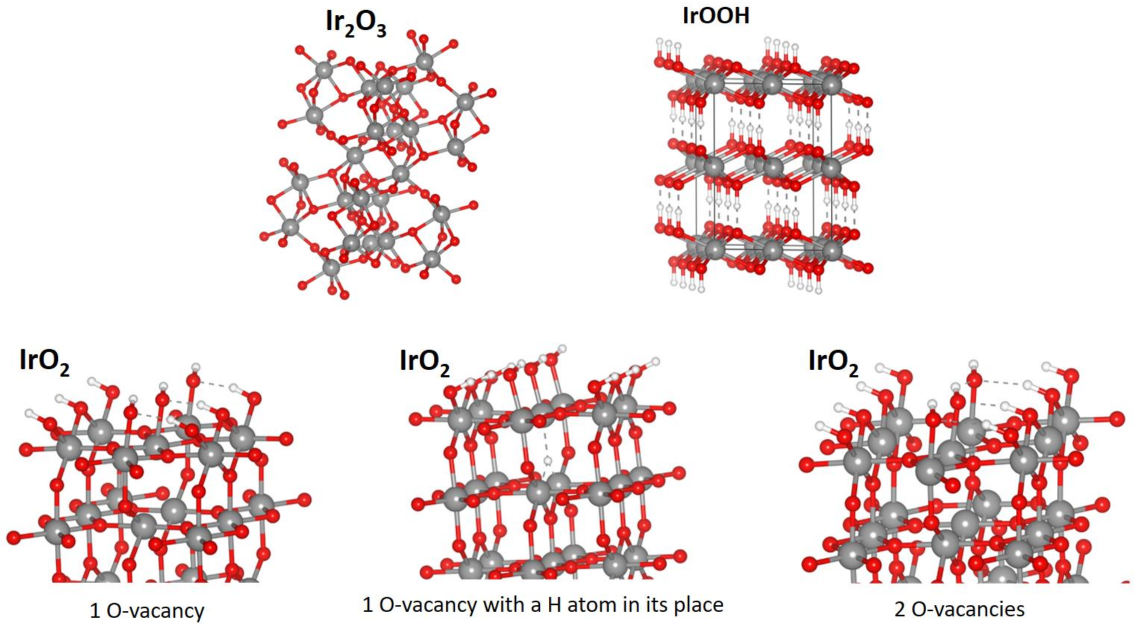

1 O-vacancy

1 O-vacancy with a H atom in its place

2 O-vacancies

Figure S7. Structures for Ir(III) compounds (Ir_2O_3 and IrOOH) and IrO_2 with 1 O-vacancy in the subsurface below the the coordinatively unsaturated (CUS) Ir site (by bond counting the CUS-Ir is $Ir^{3.7+}$), a H atom in the place of a subsurface O-vacancy (by bond counting the CUS-$Ir^{3.3+}$), 1 O-vacancy in the subsurface plus 1 O-vacancy in the surface (by bond counting the CUS-Ir^{3+}).

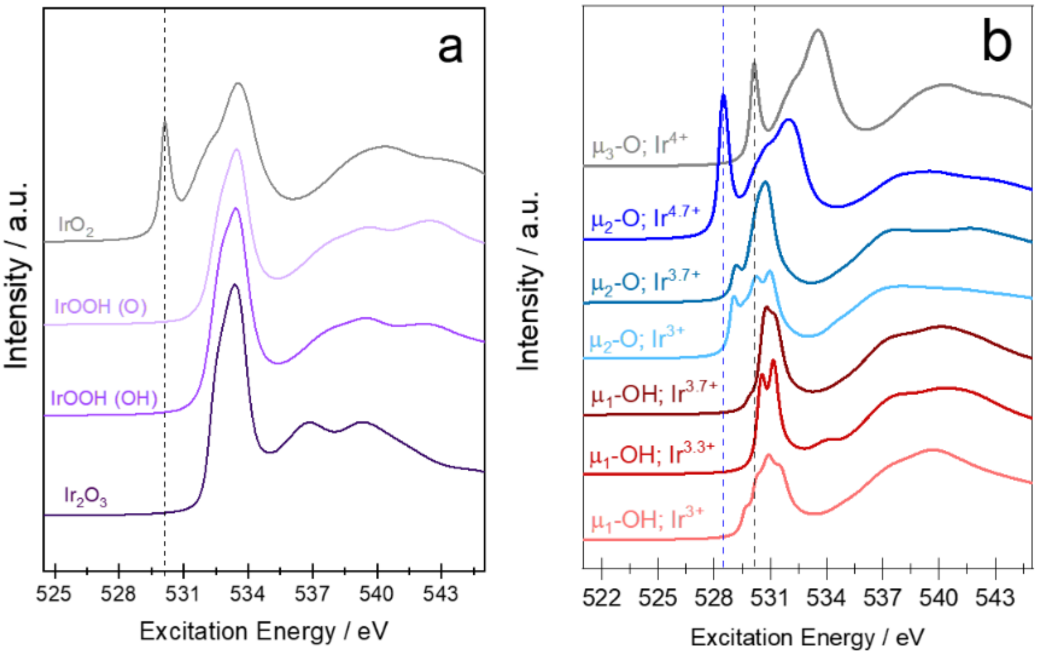

Figure S8. O K-edges computed using the single particle approach described in the main text. (a) for Ir(III) compounds and IrO_2 for comparison; note that for IrOOH oxygen is found as OH and O. (b) for different surface species on IrO_2 (110) with O-vacancies (as described and shown in Figure S7), rendering surface Ir at different oxidation states (as indicated in the figure). Oxidation states are from bond counting. The computed O K-edge spectra of μ_3-O and μ_2-O on IrO_2 without vacancies is also shown for comparison. Vertical lines indicate the resonance excitation energy for bulk μ_3-O and surface μ_2-O.

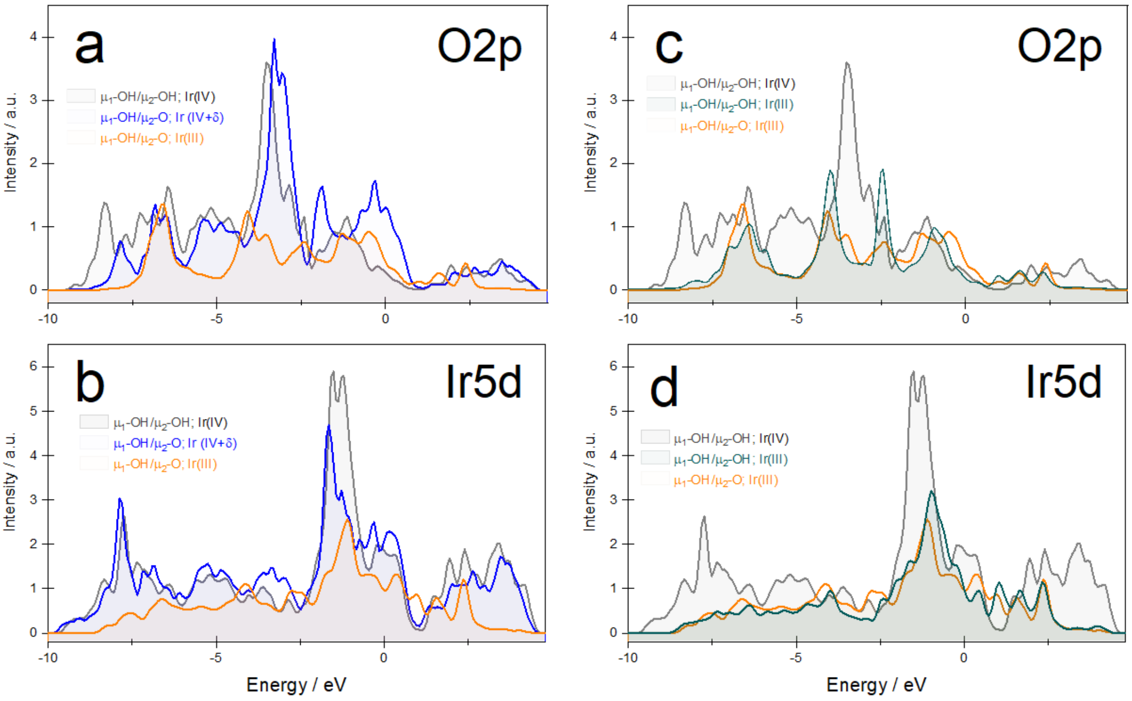

Figure S9. PDOS of O 2p (a,c) and Ir 5d (b,d) for rutile-type IrO_2 with different surface species, and IrO_2 with O-vacancies (as described and shown in Figure S7), rendering surface Ir(III), with different O-surface species. The surface Ir oxidation state is indicated in the figure.

Table S1: ΔSCF binding energies (BE) for different Ir(III) compounds and for different surface species on IrO_2 (110) with O-vacancies, and their respective Ir-oxidation state estimated from bond counting (corresponding with the structures in Figure S7). Sub-O, Sur-O and +Hsub refer to subsurface-O vacancy, surface-O vacancy and H atom in the subsurface vacancy place, respectively.

Material	Species	Vacancy	Ir -oxidation state	BE (eV)
IrO_2	bulk	----	4+	61.8
Ir2O3	bulk	----	3+	61.5
IrOOH (bulk)	bulk	----	3+	61.9
IrO_2 (110)- μ_1OH/ μ_2OH	CUS-Ir	Sub-O	3.7+	61.3
IrO_2 (110)- μ_1OH/ μ_2OH	Bridge-Ir	Sub-O	3.7+	61.6
IrO_2 (110)- μ_1OH/ μ_2OH	CUS-Ir	Sub-O; +Hsub	3.3+	61.5
IrO_2 (110)- μ_1OH/ μ_2OH	CUS-Ir	Sub-O; Sur-O	3+	61.9
IrO_2 (110)- μ_1OH/ μ_2OH	Bridge-Ir	Sub-O; Sur-O	3+	60.9
IrO_2 (110)- μ_1OH/ μ_2O	CUS-Ir	Sub-O	3.7+	61.3
IrO_2 (110)- μ_1OH/ μ_2O	CUS-Ir	Sub-O; Sur-O	3+	60.9

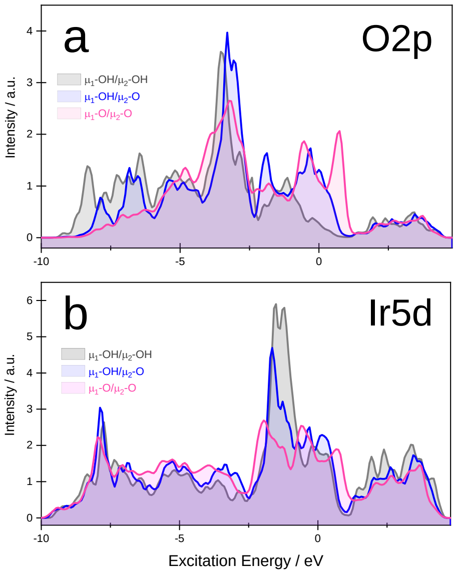

Figure S10. PDOS of O 2p (a) and Ir 5d (b) for different surface species on rutile-type IrO_2.

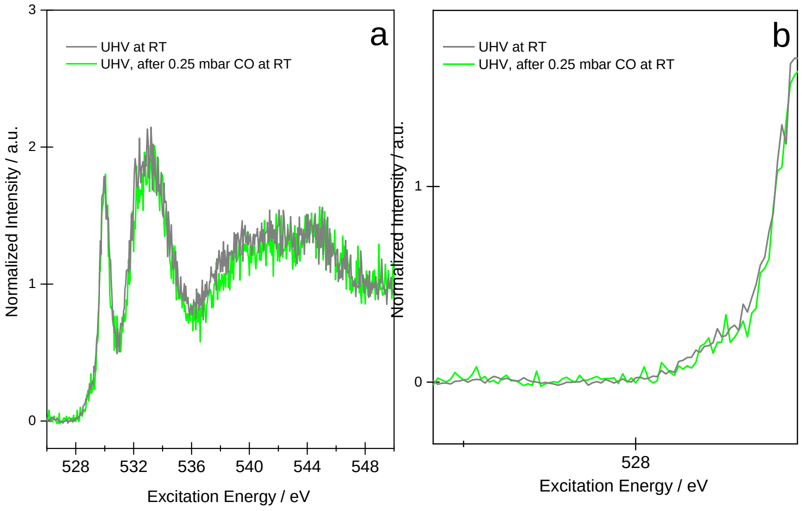

Figure S11. O K-edge of rutile-type IrO_2 in UHV at RT and after CO at RT (before CO exposure, sample was in 0.25 mbar O_2 at 573 K)

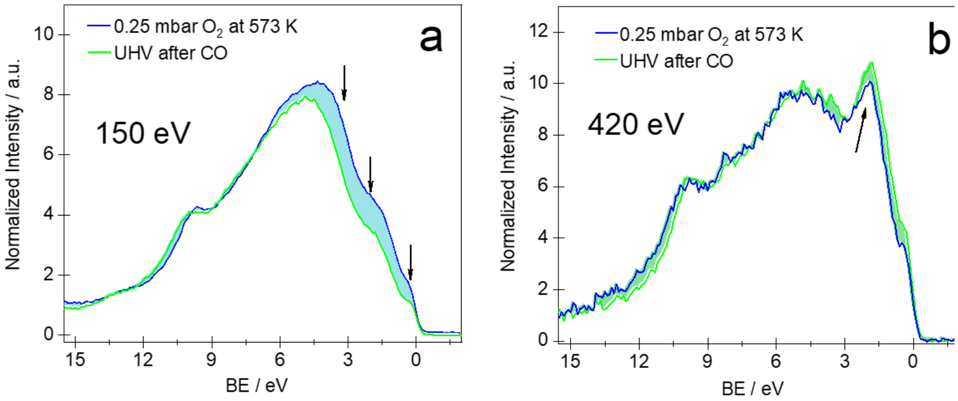

Figure S12. VB measured at 150 eV (a) and 420 eV (b) on rutile-type IrO_2 from Alfa Aesar (calcined under 1 bar O_2) Measured for the sample under 0.25 mbar O_2 at 573 K and in UHV after exposure to 0.25 mbar CO at RT.

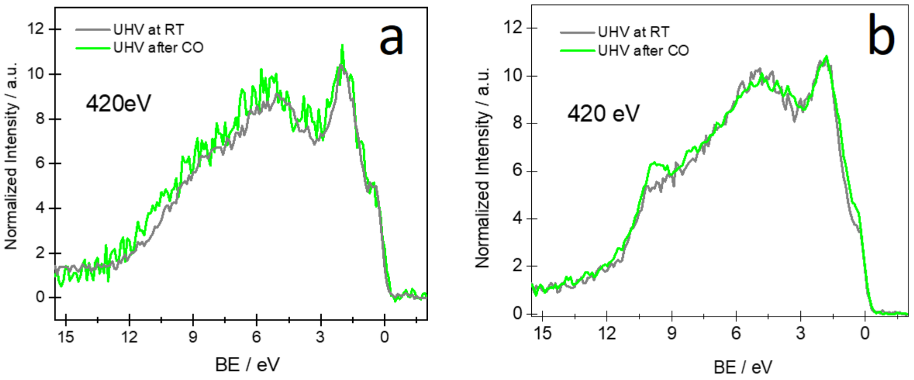

Figure S13. VB measured at 420 eV of calcined IrO_2 from Sigma Aldrich (a) and Alfa Aesar (b), in UHV as loaded and after exposure to 0.25 mbar CO at RT. The exposure to 0.25 mbar CO was done after the sample was treated under 0.25 mbar O_2 at 573 K.

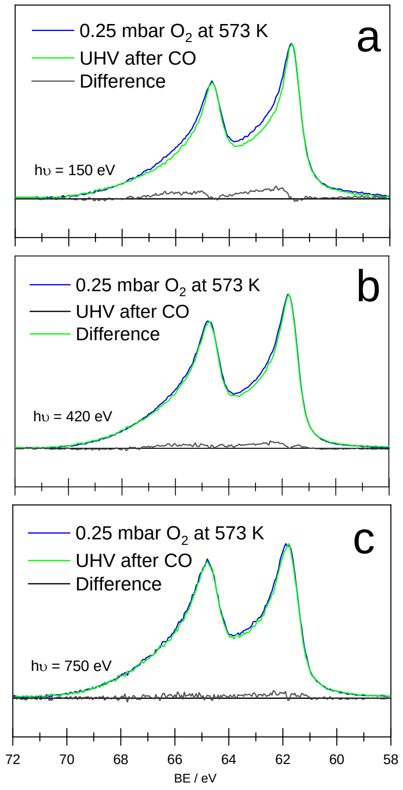

Figure S14. Ir 4f spectra of (calcined) Alfa Aesar IrO_2. Under 0.25 mbar O_2 at 573 K, after exposure to 0.25 mbar CO at RT and the respective difference spectra taken at a photon energy of (a) 150 eV, (b) 420 eV and (c) 750 eV.

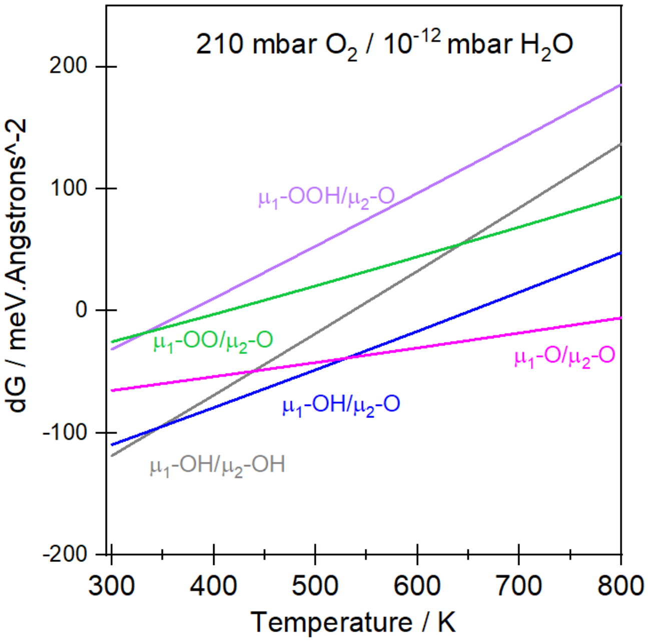

Figure S15. Calculated surface phase diagram for the surface species on rutile IrO_2 (110) under 210 mbar O_2 and 10^{-12} mbar H_2O.

References

1. Saveleva, V. A.; Wang, L.; Teschner, D.; Jones, T.; Gago, A. S.; Friedrich, K. A.; Zafeiratos, S.; Schlogl, R.; Savinova, E. R., Operando Evidence for a Universal Oxygen Evolution Mechanism on Thermal and Electrochemical Iridium Oxides. *J Phys Chem Lett* **2018,** *9* (11), 3154-3160.